Progress In Electromagnetics Research B, Vol. 31, 45–66, 2011

OPTICAL ANTIREFLECTION OF A MEDIUM BY NANOSTRUCTURAL LAYERS

A. S. Shalin †

Kotel'nikov Institute of Radio Engineering and Electronics
(Ul'yanovsk Branch)
Russian Academy of Sciences, 48 Goncharov street, Ul'yanovsk, Russia

Abstract—This work examines reflection of a light from a semi-infinite medium which is modified with an ordered monolayer of spherical nanoparticles placed on or under its surface. We derive analytical expressions for the electric fields within and outside such structures and verify them with help of strict numerical simulations. We show that nanoparticles layer acts as an imaginary zero-thickness surface having complicated non-Fresnel reflection coefficients with wavelength dependent phase shift. It is shown that such monolayers may reduce reflection relative to reflection from a pure substrate surface. We derive and analyse a zero-reflection condition in the simple intuitive form. It is shown that a single layer of nanocavities near the medium-vacuum interface may increase the transparency of a dielectric medium to values close to 100% in a wide wavelength range.

1. INTRODUCTION

At present, investigations aimed at the creation of conditionally invisible materials and media having complete or almost complete transmission of incident radiation in a given spectral range are widely performed. These investigations are stimulated by the possibility of the controlled creation and use of nanoobjects whose application makes it possible to vary the optical properties of natural materials in a sufficiently wide range by modifying the existing antireflection coatings or appropriately tuning the refractive index of the medium as a whole.

Higher light transmission of a dielectric medium is usually achieved by depositing thin-film single- or multilayer interference coatings. This approach is applicable for a sufficiently wide spectral

Received 25 March 2011, Accepted 4 May 2011, Scheduled 3 June 2011
Corresponding author: Alexander S. Shalin (shalin_a@rambler.ru).
† Also with Ul'yanovsk State University, 42 L. Tolstogo street, Ul'yanovsk, Russia.

range; however, it has substantial limitations related to necessity of depositing a great number of films of various materials with a strictly specified thickness [1] and optical properties [2, 3]. It is determined by the fundamental principle of interference minimum requiring two interfering waves to be phase-shifted by π relative to each other. These factors limit the transparency to at most 99.8%–99.9% [1]. A larger part of presently employed antireflection coatings has not so high transparency and exhibits dichroism as well [4]. In the infrared and microwave ranges, ferroelectrics and semiconductors have a sufficiently high refractive index, which hinders creation of antireflection coatings for them. Hence, a search for alternative antireflection methods capable of obtaining higher transmission in the visible spectral range becomes a necessity.

Last years a new type of antireflection coatings is being intensively developed [5–11]. It appears to be discrete nanostructured layers placed on or under the surface of a medium to be made antireflected. In [12], it is shown that the reflective capability of the substrate with a "nap" of the SiO_2 and TiO_2 nanotubes deposited on it may be reduced down to 0.05% at certain wavelengths. A similar effect was also observed in arrays of carbon nanotubes [13] and is related to light "trapping" in a sparse chaotic nanostructured material. The possibility of the achievement of the absolute transparency of medium at a given wavelength owing to the deposition of an ordered layer of spherical nanoclusters was theoretically predicted in [14, 15]. Yanagishita et al. [16] experimentally investigated the reduction of the reflection by ordered nanocrystals using the example of the layer of polymer nanocones on the surface of a lens.

A monolayer of spherical clusters was described theoretically by direct solving Maxwell's equations in spherical coordinates [17, 18]. Although the solution obtained by Mie [19] refers to diffraction from a single sphere, it can be generalized to any number of interacting particles using 3j symbols and Clebsch-Gordan coefficients, which allow one to take into account multiple coherent light scattering by nanoclusters in the structures in question [17]. This approach is however not always appropriate. Indeed, as shown earlier [17, 18, 20, 21] the interaction between particles is long-ranged and requires taking into account a rather large number of elements that influence each other. The problem can thus be treated in this approach only numerically, which requires a long computation time. Similar difficulties are encountered in other methods that directly solve Maxwell's equations, such as the finite element method (FEM) [22–24], finite-difference time-domain (FDTD) method [25, 26], small perturbation method (SPM) [27]. Moreover, taking into account

the interaction between a layer of nanoparticles and the substrate adds considerable complexity to the computation process or requires a number of approximations, e.g., averaging of the refractive indices of the substrate and environment [28], which can be done by different procedures, or the introduction of an imaginary nanostructured layer, a reflection of the real layer [18].

A recently proposed theoretical approach [15, 20, 29] allows one to find a relatively simple analytical solution to the problem of light scattering by a system of nanoclusters in the long-wavelength approximation. The theory relies on an integral-equation formalism [17, 30–32], does not require Maxwell boundary conditions for evaluating the interaction parameters of nanoparticles in the layer and, as will be shown below, makes it possible to directly take into account the mutual polarization of the medium and nanostructured layer. Note that the ability to find an analytical solution is essential for inverse optical problems, where the resultant optical properties are given *a priori*, whereas the underlying geometric and material parameters of the system are unknown. In this context, we propose to use the above-mentioned integral-equation method and to refine the results by electrodynamic finite element simulations in the COMSOL Multiphysics environment [33].

This work focuses on the interference interaction of an ordered monolayer of spherical nanoparticles with the substrate. The expressions obtained for the fields within and outside the system are used to examine the conditions under which its reflectance decreases. We derive and analyze the condition for the complete elimination of reflection from a medium (zero-reflection condition), which determines the geometric and material parameters of the nanoparticle monolayer necessary for suppressing the reflection, and demonstrate that near-zero reflection is possible for a wide wavelength range.

2. CONSTITUTIVE EQUATIONS

Let us consider the structure shown on Fig. 1, and consisting of spherical nanoparticles and a substrate. The layer and substrate are infinite in the xy plane. To assess the electromagnetic response of the system, we use the integral-equation formalism [15, 17, 20, 21] that was applied earlier to study a variety of nanostructured arrays. Here we restrict consideration to a linear approximation: the polarizations of a medium and particles are linear functions of field strength.

In this approach, the field at each point of space can be written

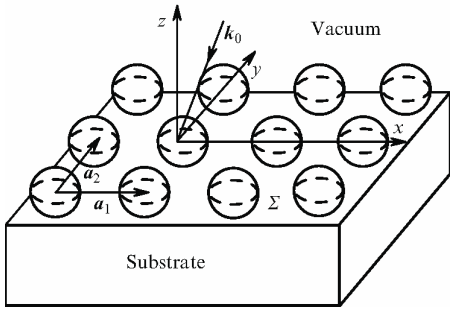

Figure 1. Geometry of the system. A wave with wave vector $\vec{k}_0$ is incident from vacuum on a surface, Σ, covered with an ordered layer of nanoparticles.

in the form:

$$\begin{aligned}&\vec{E}(\vec{r},t)\\ &= \vec{E}_I(\vec{r},t) + \int\limits_V \left\{\vec{\nabla}\times\vec{\nabla}\times\frac{\vec{P}\,(\vec{r}\,',t-R/c)}{R}\right\}dV'\\ &\quad+\frac{3}{4\pi}\sum_{j=1}^{N}\int\limits_{V_j}\left\{\vec{\nabla}\times\vec{\nabla}\times\left(\frac{\varepsilon_j\,(\vec{r}\,'_j)-1}{\varepsilon_j\,(\vec{r}\,'_j)+2}\frac{\vec{E}\,'_{j\mathit{eff}}\,(\vec{r}\,'_j,t-R'_j/c)}{R'_j}\right)\right\}dV'_j, \quad (1)\end{aligned}$$

where $\vec{E}_I(\vec{r},t) = \vec{E}_{0I}\exp(i\vec{k}_0\vec{r}-i\omega t)$ is the wave at a point of observation with radius vector $\vec{r}$ the first integral represents the response of the substrate, whose polarization $\vec{P}$ is proportional to the amplitude of the incident field; $R = |\vec{r}-\vec{r}\,'|$ is the distance from an integration point (radius vector $\vec{r}\,'$) in the medium to the point of observation; V is the volume of the medium; c is the speed of light in vacuum; and $(t-R/c)$ represents the time delay of the corresponding quantity. The second integral (more precisely, the sum of integrals) represents the field of the layer of N spherical nanoparticles, which have a complex relative dielectric permittivity $\varepsilon_j(\vec{r})$ and volume V_j, $R_j = |\vec{r}-\vec{r}\,'_j|$ and $\vec{r}\,'_j$ is the radius vector of an integration point inside the jth nanoparticle. The effective field $\vec{E}\,'_{j\mathit{eff}}$ in (1) differs from the incident plane wave $\vec{E}_I$ and has the form of a wave acting on each point in the jth nanoparticle, with allowance for the fields reemitted by the nanoparticles and substrate. As shown earlier [30, 34], $\vec{E}\,'_{j\mathit{eff}}$ comprises two contributions: external, due to the environment (the other particles of the monolayer and the substrate), and internal,

which determines the interatomic interaction in the nanoparticle and the permittivity of the particles' material. Taking into account the internal field leads to separation of (1) into local and nonlocal parts, as described in detail elsewhere [30]. The former part reduces to the Lorentz-Lorenz formula, which relates the permittivity of a particle to the polarizability and concentration of its constituent atoms. The boundary problem is thus reduced to solving nonlocal equations, namely, to finding the fields $\vec{E}_{jeff}$ that act on the nanoparticles from the environment.

For simplicity, consider a layer of identical homogeneous nanoclusters ($\varepsilon = \varepsilon_j$, $a = a_j$ $(j = 1, \ldots, N)$) using the long-wavelength approximation, which can be represented by the conditions

$$k_0 a,\ k_0 a \mathrm{Re}(n),\ k_0 a\, \mathrm{Im}\,(n) \ll 1 \tag{2}$$

where $\vec{k}_0$ is the wave vector of the incident wave, and a, $n = \sqrt{\varepsilon}$ are the radius and refractive index of the spherical clusters, respectively. With these conditions met, $\vec{E}_I$ and $\vec{E}_{jeff}$ can be considered constant throughout a given cluster and equal to those in its centre.

Placing the point of observation and the origin in the centre of the ith particle, we write the nonlocal part of Equation (1) in the form

$$\begin{aligned} &\vec{E}_{ieff} \\ &= \vec{E}_I(0,t) + \frac{3}{4\pi}\frac{\varepsilon-1}{\varepsilon+2}\sum_{\substack{j=1,\\ j\neq i}}^{N}\int_{V_j}\left\{\vec{\nabla}\times\vec{\nabla}\times\frac{\vec{E}_{jeff}\left(\vec{r}'_j, t-|\vec{r}'_j|/c\right)}{|\vec{r}'_j|}\right\}dV'_j \\ &\quad + \left(\hat{G}\vec{E}_m\right)_{(t-|\vec{\Delta}|/c)}. \end{aligned} \tag{3}$$

The second term in the right-hand side of Equation (3) represents the superposition of the fields produced by the nanoparticles in the centre of the ith particle. The third term represents the total field (with allowance for the contribution from the monolayer) reflected from the substrate surface, where $\hat{G}$ is the reflection coefficient; $\vec{E}_m$ is the effective field incident on the substrate; and $(t - |\vec{\Delta}|/c)$ is the time delay by $|\vec{\Delta}|/c$, equal to the time it takes the wave to travel from the plane defined by the centers of the nanoparticles to the substrate surface, and $\vec{\Delta} = (0, 0, -a)$. Taking into account the self-polarization of the layer through the reflection of its field from the substrate surface is of key importance because neglecting this effect leads to considerable deviations from the exact solution; $\vec{E}_m$ can be found from the nonlocal part of Equation (1), by writing it for a point of observation on the

substrate surface:

$$\vec{E}_m = \vec{E}_I\left(\vec{\Delta}, t\right) + \frac{3}{4\pi}\frac{\varepsilon-1}{\varepsilon+2}\sum_{j=1}^{N}\int_{V_j}\left\{\vec{\nabla}\times\vec{\nabla}\times\frac{\vec{E}_{j\,eff}\left(\vec{r}'_j, t-\left|\vec{\Delta}-\vec{r}'_j\right|/c\right)}{\left|\vec{\Delta}-\vec{r}'_j\right|}\right\}dV'_j. \quad (4)$$

Equations (3) and (4) constitute a self-consistent system of integral equations, whose solution is the effective electric field in the monolayer. Unfortunately, the reflection coefficient $\hat{G}$ is rather difficult to calculate in general form [35]. In particular, the standard procedure based on the extinction theorem in integral form [30] cannot be used to perform the integration over the medium in (1) because the field produced by the nanoparticles in the surface layer of the substrate is inhomogeneous. The solution can then be found using the above-mentioned coupled dipole method, which requires purely computational means. On the other hand, as we showed previously [29] the reflection coefficient $\hat{G}$ of an inhomogeneous field can be approximated by a tensor constructed from the Fresnel reflection coefficients for a plane wave. In the optical region, this approximation is applicable when the characteristic values of the geometric parameters of the metalayer (lattice period and particle size) do not exceed a few tens of nanometres at a moderate absorption coefficient of the particles, which corresponds to conditions (2). The $\hat{G}$ tensor then has the form

$$\hat{G} = \begin{bmatrix} r_\perp \sin^2\varphi - r_{||}\cos^2\varphi & -\left(r_\perp + r_{||}\right)\sin\varphi\cos\varphi & 0 \\ -\left(r_\perp + r_{||}\right)\sin\varphi\cos\varphi & r_\perp\cos^2\varphi - r_{||}\sin^2\varphi & 0 \\ 0 & 0 & r_{||} \end{bmatrix},$$

where $r_\perp, r_{||}$ are the Fresnel reflection coefficients for the electric vector components normal and parallel to the plane of incidence [30] and φ is the angle between the plane of incidence and the x axis.

3. OPTICAL FIELDS IN THE NANOSTRUCTURED LAYER

Consider the field produced by the jth nanoparticle in vacuum at a point of observation with radius vector $\vec{R}$ outside the nanoparticle. In the long-wavelength approximation, the integral representing the field strength in (1) can be calculated easily by the Ewald-Oseen method [30], as done in previous studies [20, 21, 36]. As a result, we

obtain the relation

$$\vec{E}_{j\,sca}\left(\vec{R}\right) = \alpha_p \hat{f}_j\left(R\right)\vec{E}_{j\,eff}, \quad \alpha_p = a^3\frac{\varepsilon-1}{\varepsilon+2}, \tag{5}$$

where the $\hat{f}_j(R)$ tensor has the following components for the external field polarizations parallel and normal to $\vec{R}$:

$$\begin{aligned} f_j^P\left(R\right) &= \exp\left(ik_0R\right)\left(\frac{2}{R^3}-\frac{2ik_0}{R^2}\right), \\ f_j^S\left(R\right) &= \exp\left(ik_0R\right)\left(-\frac{1}{R^3}+\frac{ik_0}{R^2}+\frac{k_0^2}{R}\right), \end{aligned} \tag{6}$$

According to Equations (5) and (6), the field scattered by a nanoparticle strictly corresponds to that created by a dipole of polarizability α_p located in the centre of the particle [30, 34]. Clearly, if the particle is surrounded not by vacuum but by the medium with dielectric permittivity $\tilde{\varepsilon}_m$, the permittivity ε in (5) is relative rather than absolute, and k_0 must be replaced by $k = k_0\sqrt{\tilde{\varepsilon}_m}$.

Let us use the principle of parallel translational symmetry [37, 38], according to which an electric field (an external wave or the wave reflected from the substrate surface) incident on a layer of nanoparticles meets the condition

$$\vec{E}_{inc}\left(\vec{r}_j\right) = \vec{E}_{inc}\left(0\right)\exp\left(i\vec{q}\vec{r}_j\right), \tag{7}$$

Here, $\vec{r}_j$ is the radius vector of the centre of the jth nanoparticle, and the components of the $\vec{q}$ vector are $(q_x, q_y, 0)$, where $q_x = k_{0x} = k_0\sin\theta_I\cos\varphi$ and $q_y = k_{0y} = k_0\sin\theta_I\sin\varphi$ (θ_I is the angle of incidence). Therefore, since all the clusters are identical, the field amplitudes are $\vec{E}_{j\,eff} = \vec{E}_{i\,eff} = \vec{E}_{eff}$ and the phase shift is given by (7). With Equations (5)–(7), the integrals in (3) and (4) can be converted to lattice sums:

$$\begin{aligned} &\frac{3}{4\pi}\frac{\varepsilon-1}{\varepsilon+2}\sum_{j=1}^{N}\int\limits_{V_j}\left\{\vec{\nabla}\times\vec{\nabla}\times\frac{\vec{E}_{eff}\left(\vec{r}_j', t-R_j'/c\right)}{R_j'}\right\}dV_j' \\ &= \alpha_p\vec{E}_{eff}\sum_{j=1}^{N}\hat{f}_j\left(|\vec{r}-\vec{r}_j|\right)\exp\left(i\vec{q}\vec{r}_j\right). \end{aligned} \tag{8}$$

Therefore, the system of integral Equations (3) and (4) reduces to the following linear algebraic equation for the field acting on a cluster:

$$\vec{E}_{eff} = \vec{E}_I(0) + \alpha_p\vec{E}_{eff}\hat{A}_p + \hat{G}\left[\vec{E}_I(0)\exp\left(2i\vec{k}_0\vec{\Delta}\right) + \left(\alpha_p\vec{E}_{eff}\hat{C}_p^{-}\left(2\vec{\Delta}\right)\right)\right], \tag{9}$$

where the term in square brackets is equal to $(\vec{E}_m)_{(t-|\vec{\Delta}|/c)}$ given that the wave reflected from the substrate lags the wave incident on the layer both in the path from the plane defined by the centers of the nanoparticles to the substrate surface and after the reflection, in the path from the substrate surface to that plane. In (9), we use the following designations:

$$\hat{A}_p = \sum_{\substack{j=1,\\ j\neq i}}^{N} \hat{f}_j\left(|\vec{r}_j|\right)\exp\left(i\vec{q}\vec{r}_j\right), \tag{10}$$

is the lattice sum determining the field produced at the ith particle by the other particles in the layer and

$$\hat{C}_p^{-}\left(2\vec{\Delta}\right) = \left(\sum_{j=1}^{N} \hat{f}_j\left(\left|\vec{\Delta}-\vec{r}_j\right|\right)\exp\left(i\vec{q}\vec{r}_j\right)\right)_{(t-|\vec{\Delta}|/c)} \tag{11}$$

is the lattice sum describing the field emitted by the layer towards the substrate (the superscript "$-$" denotes that the wave propagates in the negative direction relative to the z axis). The calculated lattice sums of the form (10) and (11) are given in the Appendix.

Solving Equation (9) for the effective field acting on a nanoparticle in the monolayer, we obtain

$$\vec{E}_{eff}\left(0\right) = \frac{1+\hat{G}\exp\left(2i\vec{k}_0\vec{\Delta}\right)}{1-\alpha_p\hat{A}_p-\hat{G}\left(\alpha_p\hat{C}_p^{-}\left(2\vec{\Delta}\right)\right)}\vec{E}_I(0). \tag{12}$$

The effective-polarizability approach allows one to deal with the external field strength without considering the parameters of the structure. From the relation

$$\vec{d}_p = \alpha_p\vec{E}_{eff} = \hat{\alpha}_{peff}\vec{E}_I, \tag{13}$$

where $\vec{d}_p$ is the dipole moment of a nanocluster, we obtain the following formula for the effective polarizability of the nanoparticle:

$$\hat{\alpha}_{peff} = \alpha_p\frac{1+\hat{G}\exp\left(2i\vec{k}_0\vec{\Delta}\right)}{1-\alpha_p\hat{A}_p-\hat{G}\left(\alpha_p\hat{C}_p^{-}\left(2\vec{\Delta}\right)\right)}. \tag{14}$$

4. REFLECTED WAVE FIELD IN THE WAVE ZONE. EFFECT OF A MONOLAYER OF PARTICLES ON REFLECTANCE

At a point of observation with radius vector $\vec{p}$, the wave reflected from a monolayer-substrate system has the form

$$\vec{E}_{refl}(\vec{p}) = \left\{\hat{G}\exp\left[i\vec{k}_0\vec{\Delta} + i\vec{k}_0^R\left(-\vec{\Delta}+\vec{p}\right)\right] + \hat{\alpha}_{peff}\left[\hat{G}\hat{C}_p^-\left(2\vec{\Delta}-\vec{p}\right) + \hat{C}_p^+(\vec{p})\right]\right\}\vec{E}_I, \quad (15)$$

where the use of $-\vec{p}$ in $\hat{C}_p^-(2\vec{\Delta}-\vec{p})$ allows us to avoid dividing the wave path into two parts (in the $-z$ direction from the layer to the substrate surface and then in the opposite direction from the substrate to point $\vec{p}$) and to replace it with the total distance plotted in the z direction, and $\vec{k}_0^R = (k_{0x}, k_{0y}, -k_{0z})$ is the wave vector of the reflected wave.

It follows from (15) that the reflected wave amplitude is the sum of three quantities. One of them, the first term in (15), represents Fresnel reflection from a pure substrate without nanoparticles. The other two terms are due to the polarization of the nanospheres, which interact electrodynamically with one another and with the substrate: $\alpha_{peff}\hat{C}_p^+(\vec{p})\vec{E}_I$ represents the emission from the monolayer in the reflected wave direction ($+z$ direction) and $\alpha_{peff}\hat{G}\hat{C}_p^-(2\vec{\Delta}-\vec{p})\vec{E}_I$ represents the emission from the monolayer to the substrate reflected from its surface. Since the phase factors of these terms depend significantly on the geometry and material parameters of the monolayer substrate system, interference of the corresponding waves at the point of observation may raise or reduce the reflection coefficient relative to the Fresnel coefficient.

In certain cases, expression (15) can be substantially simplified. We have shown in [29] that, for the considered system, the following condition is well satisfied in the optical range (see Appendix):

$$\frac{\left|\hat{C}_p^{01}(\vec{r})\right|}{\left|\hat{C}_p^{00}(\vec{r})\right|} << 1, \quad (16)$$

In this situation, only the first nonevanescent harmonic can be retained in the decomposition of the field scattered by a nanoparticle layer. The above inequality holds when the characteristic geometric parameters of a metalayer (lattice period, particle dimension) have values of about several tens of nanometers. As it is seen from the Appendix and studies [14, 29], it is necessary to take into account

nonzero decaying harmonics in lattice sum $\hat{C}_p^{\pm}$ only in the case of large values of lattice constants, small radii of particles, or large wavelengths. So, we can express lattice sum (11) as follows (see Appendix):

$$\hat{C}_p^{\pm}(\vec{r}) = C_n \exp\left(\mp i\vec{k}_0\vec{r}\right), \quad C_n = \frac{\vec{E}_I}{\left|\vec{E}_I\right|} \cdot \frac{2\pi i k_0^2}{|\vec{a}_1 \times \vec{a}_2|\, k_{0z}}, \tag{17}$$

where k_{0z} is the z component of the wave-vector, $\vec{a}_1$, $\vec{a}_2$ are the vectors of the lattice constants of the layer. With allowance for (17), expression (15) can readily be modified into the form

$$\hat{r} = \frac{\vec{E}_{refl}(0)}{\vec{E}_I(0)} = \frac{\hat{R}_l + \hat{R}_{12}\exp\left\{2i\left(\vec{k}_0\vec{\Delta}\right)\right\}}{1 - \hat{R}_{21}\hat{R}_l\exp\left\{2i\left(\vec{k}_0\vec{\Delta}\right)\right\}}, \tag{18}$$

which corresponds to the Airy reflection coefficient for a film located on the surface of an underlying medium. Here,

$$\hat{R}_l = \frac{\alpha_p C_n}{1 - \alpha_p \hat{A}_p} \tag{19}$$

is the tensor of the non-Fresnel reflection coefficients of the metalayer. In a similar manner, we can obtain the system's transmission coefficient that describes the total field transmitted into the substrate:

$$\hat{t} = \frac{\vec{E}_{tran}\left(\vec{\Delta}\right)}{\vec{E}_I(0)} = \frac{\hat{T}_{12}\hat{T}_l\exp\left\{i\left(\vec{k}_0\vec{\Delta}\right)\right\}}{1 - \hat{R}_{21}\hat{R}_l\exp\left\{2i\left(\vec{k}_0\vec{\Delta}\right)\right\}}, \tag{20}$$

where the tensor of the non-Fresnel transmission coefficients of the metalayer has the form

$$\hat{T}_l = 1 + \frac{\alpha_p C_n}{1 - \alpha_p \hat{A}_p}. \tag{21}$$

Tensors (19) and (21) have similar forms, because the metalayer field is symmetric with respect to the plane where the layer is located (see Appendix).

Thus, the monolayer of the nanoparticles is an imaginary interface between two media, which passes through the centers of the clusters and has complicated reflection and transmission coefficients. In other words, the system under consideration can be represented as a film with the thickness Δ (the distance from the surface of the matrix medium to the imaginary interface) that is located on the surface of the semi-infinite substrate. It is worth noting that the layer of nanoparticles (or an ordered aggregate of several layers) was treated

in some papers (see f. e. [39]) as a finite-thickness film with a certain effective refractive index different from the refractive index of the matrix medium, as in the Maxwell-Garnett effective medium theory [40]. However, in view of the absence of the pronounced boundaries of the layer which can be treated as the boundaries of this film, the different thicknesses of this film were determined in different works. This difficulty is easily understood considering the monolayer consisting of micellar nanoobjects, which are nuclei covered by needlelike outgrowths rather than of spherical particles. In this case, it is unobvious whether the thickness of this heterogeneous film should be defined as the diameter of the nucleus or micellar needles should be included into the film. One of the variants of the definition of the thickness is the definition of the fictitious boundaries at which the wave scattered by the layer becomes plane (all of the evanescent harmonics caused by the discrete structure of the layer and by the shape of the constituent nanoparticles are damped). Since the ratio of the total volume of the nanoparticles to the total volume of the film (filling factor) obviously depends on the definition of the boundaries of the composite film, the effective refractive index is a nonlinear function of the thickness, thus strongly affecting the resulting optical properties of the system. In the framework of the presented formalism, the indicated difficulties are absent, because the parameters are not averaged. In this case, the extinction theorem is also satisfied, because the separation of the incident wave into the reflected and transmitted waves, whose amplitudes are determined by the tensor coefficients given by Equations (19) and (21), occurs exactly on the plane passing through the centers of the nanoparticles.

Taking into consideration simple form of Equations (18), (20) it is possible to obtain corresponding formulas for "inverted" system when nanoparticles layer is embedded into a substrate with refractive index $\tilde{n}_m = \sqrt{\tilde{\varepsilon}_m}$ without any additional calculations. The reflection coefficient of such a structure has the following form:

$$\hat{r} = \frac{\hat{R}_{12} + \hat{R}_l \exp\left\{2i\left(\vec{k}\vec{\Delta}\right)\right\}}{1 - \hat{R}_{21}\hat{R}_l \exp\left\{2i\left(\vec{k}\vec{\Delta}\right)\right\}}, \tag{22}$$

where $\vec{k} = \vec{k}_0\tilde{n}_m$ is the wave vector in a substrate, $\hat{R}_l$ depends on $\vec{k}$, and transmission coefficient $\hat{t}$ has the form of (20) with the following replacement $\vec{k}_0 \to \vec{k}$.

5. CONDITION OF THE TOTAL BLOOMING OF A SUBSTRATE

The following condition under which the medium becomes absolutely transparent due to nanolayer on its surface can be obtained from Equations (18), (22), where the reflection coefficient is set to zero:

$$\hat{R}_l = -\hat{R}_{12} \exp\left\{\pm 2i\left(\vec{k}\vec{\Delta}\right)\right\}, \tag{23}$$

where the left- and right-hand sides characterize the layer of the nanoparticles and the substrate, respectively. Phase shift $2i(\vec{k}\vec{\Delta})$ has sign "+", and $\vec{k} = \vec{k}_0$ if the nanolayer is on the surface of a medium; and sign "−", and $\vec{k} = \vec{k}_0\tilde{n}_m$ if it is imbedded into a medium. The form of Equation (23) is well known in the optics of antireflection coatings; this condition is formally separated into two conditions, the first of which requires the equality of the reflection coefficients of the film and substrate and the second, the presence of a path difference of $\lambda/2$ (where λ is the wavelength in the surrounding medium) between the reflected waves.

$$\left|\hat{R}_{12}\right| = \left|\hat{R}_l\right|, \tag{24a}$$

$$\exp\left\{2i\left(\vec{k}\vec{\Delta}\right) \pm i\left(-\rho_l + \rho_{12}\right) + i\pi\right\} = -1, \tag{24b}$$

where ρ_{12} and ρ_l are the arguments of $\hat{R}_{12}$ and $\hat{R}_l$, respectively. Since the bloomed medium is a dielectric material with the refractive index > 1, it is obvious that $\rho_{12} = \pi$.

Figure 2 shows the reflection spectra of the system under consideration obtained by exact electrodynamic finite element computations [33]. We used about 10^5 mesh elements in our geometry (Fig. 1) to achieve the precision $10^{-3}\%$ while calculating reflection and transmission spectra. The refractive index of the substrate was chosen so as to meet condition (23) at wavelengths of 550 (Fig. 2(a)) and 460 nm (Fig. 2(b)), and the parameters of the monolayer were set *a priori*. The material of the nanoparticles in Fig. 2(a) is a hypothetical medium with a refractive index $n = 1.8$, and that in Fig. 2(b) is silicon, with the known dispersion of its optical constants [41].

Note that in Fig. 2 the reflectance does not become zero at the minima (but the minimum reflectance is several hundred times lower than the reflectance of an uncoated substrate surface), and the minima are slightly shifted from the intended 550 and 460 nm, which is due to the discrepancy between the analytical solution (which was used to derive condition (23)) and the exact solution [29]. Therefore, in the case of large ($a \geq 20$ nm [29]) nanoparticles, the refractive index of

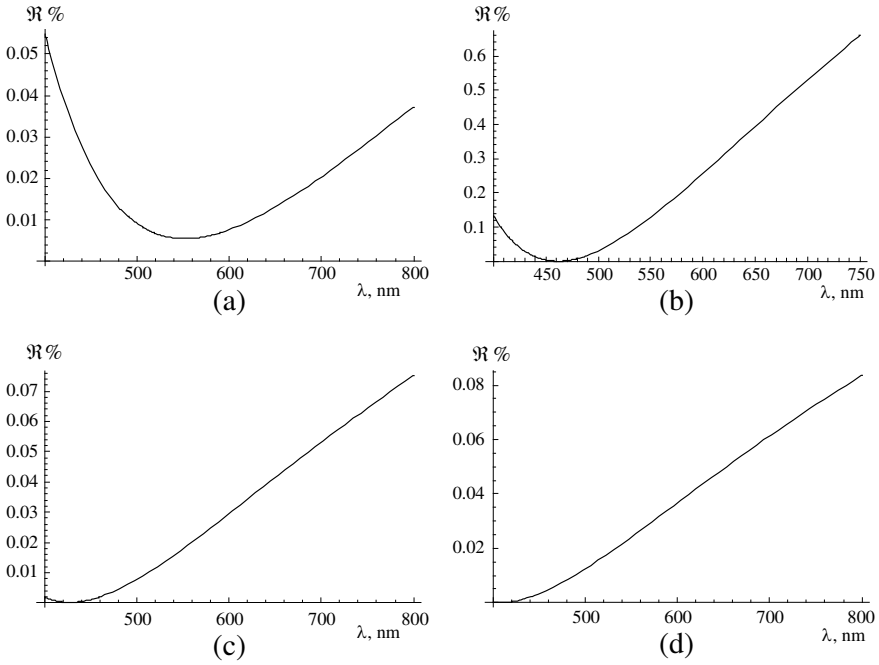

Figure 2. Reflection ($\Re$) spectra of a system comprising a monolayer of spherical nanoparticles and a substrate: (a) $a = 15\,\text{nm}$, $n = 1.8$, $\tilde{n}_m = 1.03 + 0.11i$; (b) $a = 20\,\text{nm}$, $n = n(\omega)$ (silicon), $\tilde{n}_m = 1.23 + 0.33i$; y-axis polarized wave is incident on the system along the normal to its surface ($\theta_I = 0$). The particles are arranged in the form of a square lattice with periods $|\mathbf{a}_{1,2}| = 3a$. (c) and (d) are given to illustrate the effect of lattice form on the reflection spectra, parameters of particles and substrate are the same as on Fig. 2(a) and lattice constants: (c) $|\mathbf{a}_1| = 4a$, $|\mathbf{a}_2| = 3a$; (d) $|\mathbf{a}_1| = 3a$, $|\mathbf{a}_2| = 4a$.

the substrate found from (23) must also be slightly corrected using the exact solution. In this work, this was done by adjusting the corresponding parameter. In particular, the analytical refractive index of the substrate, $\tilde{n}_m$, in Fig. 2(b) is $1.1 + 0.36i$, whereas the minimum in reflectance is reached at $1.23 + 0.33i$. This is because condition (2) is not met, and the particles no longer behave as dipoles localized at their centre, so multipole terms in the expansion of the scattered field must be taken into account.

It should also be emphasized that reflection suppression is significant (by more than a factor of 10) in a rather broad wavelength range: from 460 to 800 nm in Fig. 2(a) and from 400 to 600 nm in

Fig. 2(b). Moreover, there is no absorption in the layer in Fig. 2(a), and the average absorptance in the visible range in Fig. 2(b) is 0.13%.

The optical response of a coating composed of nanoparticles can be tuned by varying the internal geometric parameters. For example, at a fixed refractive index of the substrate, changing the particle radius by 1% shifts the minimum in reflectance by approximately 27 nm in Fig. 2(a) and 23 nm in Fig. 2(b). Reducing the particle size shifts the minimum to shorter wavelengths, and vice versa. The lattice constant also influences the position of the zero-reflection region: with decreasing lattice density, it shifts to shorter wavelengths (see Figs. 2(c), (d)). Moreover, variation of the lattice constant which is parallel to the incident wave polarization affects spectra greater (Fig. 2(d)). If we fix not the optical constants of the substrate but the zero-reflection wavelength, the parameters of the monolayer at which condition (23) is met depend on the substrate, with the following relationship: the higher the reflectance of the substrate, the higher must be the effective optical density of the metalayer (denser packing, larger particles or higher optical density of the particles). This conclusion is obvious because the wave generated by the monolayer then has a larger amplitude and, accordingly, suppresses the stronger reflection from the substrate through destructive interference.

It is worth noting that total antireflection takes place only for media with refractive index close to unity. This is because of condition (24b) which can not be satisfied if particles are on a substrate and have radii about tens nanometers. Parameter Δ is much smaller then $\lambda/4$ in this case and corresponding phase shift $2(\vec{k}\vec{\Delta}) \ll \pi$. On the other hand if nanoparticles' layer is embedded into a substrate, its reflectance decreases (because of decreasing particles polarizability α_p (5)), but the condition of an interference minimum of reflection, which can be easily obtained from Equation (22) and is similar with (24b), can be strictly fulfilled allowing us to achieve optical blooming for strongly refractive media.

Let us consider the optical properties of glass ($\tilde{n}_m = 1.5$) with the introduced layer of spherical nanoinclusions. According to the above-mentioned, the refractive index of the material of these nanoparticles should differs from the $\tilde{n}_m$ as much as possible to increase polarizability α_p; therefore, the layer consisting of nanocavities with $n = 1$ has the maximum reflectivity. The use of metallic nanoparticles having the refractive index with the real part smaller than unity would make it possible to additionally increase reflectivity, but the absorption of radiation in such a monolayer can reach several percent, making its application unreasonable in this case.

Assuming that the lattice constants are equal to the minimum

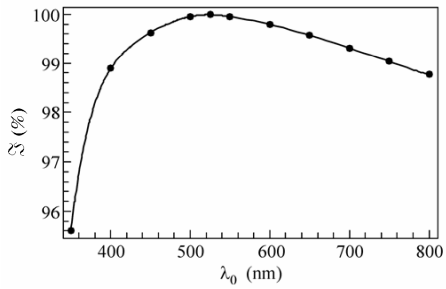

Figure 3. Transmittance of glass ($\tilde{n}_m = 1.5$) with the introduced layer of nanocavities with the radii $a = 50\,\text{nm}$. The lattice constants are the same and are equal to $2a$ (cavities are located close to each other) and the layer location depth is $\Delta = 51\,\text{nm}$. The calculation was performed by the exact electrodynamical finite element method.

value $2a$ corresponding to adjoining cavities, the radius of the cavities $a \approx 50\,\text{nm}$ necessary for the satisfaction of Equation (24a) at a wavelength of 550 nm. In this case, to calculate the reflection and transmission spectra of the system with these parameters, the exact electrodynamics finite element method [22–34] is used in order to exclude the effect of made approximation (2) and the absence of multipole terms in the nanoparticle interaction tensor (6) (which are significant for the considered case of touching spheres) on the result. According to [29], for such geometrical parameters of the nanoaggregate, the considered analytical approach can be used only for estimating investigations. Thus, the calculation of the spectral dependence of the transmissivity of the medium with the introduced layer of the nanoparticles is performed strictly with an accuracy up to 0.001%, whereas the parameters necessary for the complete blooming of the system are determined approximately in the frame of proposed method.

As is seen in Fig. 3, the transparency of the medium is indeed broadband in this case and the transmission of radiation exceeds 99% in the interval of 400–750 nm. The section of the spectral dependence of the transmissivity in which it depends slightly on the wavelength and is close to the maximum value is also sufficiently wide ($> 99.8\%$ in the interval of 470–600 nm). In this case, the transmission peak $\Im = 100\%$ is observed at a wavelength of 527 nm rather than at 550 nm, as was assumed. This is due to the mentioned discrepancy between the numerical and analytical results. Note that transmission decreases rapidly in the blue region, because the reflectivity of the layer of nanocavities, which increases with a decrease in the wavelength,

becomes too high. In view of this circumstance, it is reasonable to use larger cavities in optical media denser than glass, because reflectivity increases additionally in this case.

It is worth noting that the change in the parameters of the monolayer gives rise to the weakening of the blooming effect at Fig. 3. In particular, when the radius of the spheres decreases to 40 nm or increases to 60 nm, the region in which $\Im = 99.8\%$ is decreased by a factor of 1.5–2 and the blooming becomes more narrowband. The transmissivity with the use of the particles with $n > \tilde{n}_m$ exhibits a pronounced peak and, beyond the maximum, is smaller than the corresponding value for a pure medium. This confirms that the broadband increase in the transparency can occur only under the above conditions imposed on the material and geometric parameters of the nanolayer.

It is necessary to underline that the similar effect of broadband optical antireflection of a medium by the nano-structured layer was experimentally observed in paper [42] for the glass film coated with the layer of parabolic nano-pillars.

6. CONCLUSIONS

We examined electrodynamic interaction between an ordered monolayer of spherical nanoparticles and a substrate. The results show that, in such systems, the fields reflected from the monolayer and the substrate surface may interfere both constructively and destructively, raising or reducing the reflectance of the entire system. We derived and analyzed conditions for complete elimination of reflection from the substrate and identified the factors that influence the minimum-reflectance wavelength. Using the proposed approach and the finite element method, it has been shown that the semi-infinite medium can be bloomed in a wide wavelength range by the introduction of a single layer of nanoparticles or nanocavities. The results of this work can be significant for the development of materials with high transparency ("invisible" materials), the creation of blooming coatings with a quality higher than that of the existing materials, and an increase in the transmissivity of media whose blooming by the existing methods is difficult or impossible.

One possible application of this effect is the engineering of antireflection coatings for existing artificial media with a refractive index close to unity [43]. According to the general theory of antireflection coatings [30], the refractive index of the antireflection film should then be closer to that of vacuum, so that no natural materials can be exploited for this purpose. The use of a loose

structure with controlled optical characteristics, such as a monolayer of nanoparticles, makes it possible to substantially suppress or completely eliminate reflection from such materials, which in turn paves the way for engineering absolutely transparent materials.

APPENDIX A.

For calculation of lattice sums (10) and (11), we apply the technique proposed by Ewald and successfully used in a series of studies [37, 38]. First, let us consider the case when the observation point is beyond the layer and the layer is located in free space. Note that, if a nanoparticle monolayer is in a medium with $\tilde{n}_m \neq 1$, the replacement $\vec{k}_0 \to \vec{k}_0 \tilde{n}_m$ should be made in the formulas below. Taking into account that the function describing the dipole field is periodic and has the lattice period, we decompose this function in the Fourier series in the vectors of the reciprocal lattice. Since the expressions from the Appendix are derived in the literature cited above, we directly present the result:

$$\hat{C}_p\left(\vec{r}-\vec{r}_j\right) = -\sum_{p,q=-\infty}^{\infty} \frac{2\pi i}{\left|\vec{a}_1 \times \vec{a}_2\right|} \left[\vec{k}_{pq} \times \left(\vec{k}_{pq} \times \vec{n}_0\right)\right] \frac{\exp\left(i\vec{k}_{pq}\vec{r}\right)}{\kappa_{pq}} \quad \text{(A1)}$$

where $\vec{n}_0 = \vec{E}_I / \left|\vec{E}_I\right|$, $\kappa_{pq} = \sqrt{k_0^2 - \left(\vec{q} + \vec{g}_{pq}^{\,|}\right)^2}$ $\vec{g}_{pq}^{\,|} = p\vec{g}_1 + q\vec{g}_2$,

$$\vec{k}_{pq} = \begin{cases} \left(\vec{q} + \vec{g}_{pq}^{\,|}, \kappa_{pq}\right), & z > 0 \\ \left(\vec{q} + \vec{g}_{pq}^{\,|}, -\kappa_{pq}\right), & z < 0 \end{cases} \quad \text{(A2)}$$

The vectors of the reciprocal lattice are as follows:

$$\vec{g}_1 = 2\pi \frac{\vec{a}_2 \times \vec{n}}{\left|\vec{a}_1 \times \vec{a}_2\right|}, \quad \vec{g}_2 = 2\pi \frac{\vec{n} \times \vec{a}_1}{\left|\vec{a}_1 \times \vec{a}_2\right|}, \quad \text{(A3)}$$

where $\vec{a}_1 = (\alpha, 0, 0), \vec{a}_2 = (\beta, \gamma, 0)$ are the minimum-length translation vectors of the direct lattice and the vector $\vec{n} = (0, 0, 1)$ is perpendicular to the monolayer surface. Expression (A1) is the decomposition of the field induced by a nanoparticle monolayer in a plane harmonic wave ($p = q = 0$) and a series of exponentially decaying evanescent waves existing when $|\vec{q} + \vec{g}_{pq}| > k_0$, κ_{pq} are imaginary quantities.

Now, let us calculate lattice sum (10) for the observation points inside the metalayer. According to the Ewald method [38], we have the following expression at $z = 0$:

$$\hat{A}_p = \hat{l}\left(\vec{k}_0\right) \vec{n}_0 \exp\left(i\vec{q}\vec{r}_j\right). \quad \text{(A4)}$$

Tensor $\hat{l}$ is symmetric, contains zero components $l_{xz}, l_{yz}, l_{zx}, l_{zy}$ and has the form

$$l^{\mu\nu}\left(\vec{k}_0\right) = c^{\mu\nu} - \left[\frac{2}{3}ik_0^3\mathrm{Erfc}\left(\frac{ik_0}{2F}\right) + \frac{4F}{3\sqrt{\pi}}\left(k_0^2 - F^2\right)\exp\left(\frac{k_0^2}{4F^2}\right) - \frac{2}{3}ik_0^3\right]\delta^{\mu\nu}. \quad \text{(A5)}$$

This expression includes the complementary error function integral (Erfc), which rapidly approaches zero at large values of the argument,

$$\begin{aligned} c^{\mu\nu} = {} & \frac{i\pi}{|\vec{a}_1 \times \vec{a}_2|}\sum_{p,q}\left[\frac{k_0^2\delta^{\mu\nu} - k_{pq\nu}k_{pq\mu}}{\kappa_{pq}}\Delta_{pq}\left(1+\tau\right) + \eta\Sigma_{pq}\right] \\ & + \frac{1}{2}\sum_{n,m}\frac{\exp\left(i\vec{k}_0\vec{a}_{nm}\right)}{a_{nm}^3}\left\{\Gamma_{nm}^{(1)}\left[\delta^{\mu\nu}\Gamma_{nm}^{(2)} + \vec{a}_{nm}^{\mu}\vec{a}_{nm}^{\nu}\Gamma_{nm}^{(3)}\right]\right. \\ & \left. + \Gamma_{nm}^{(4)}\left[-\delta^{\mu\nu}a_{nm} + \vec{a}_{nm}^{\mu}\vec{a}_{nm}^{\nu}\Gamma_{nm}^{(5)}\right] + \kappa.c.\right\} \end{aligned} \quad \text{(A6)}$$

where $\mu, \nu = x, y, z, \vec{a}_{nm} = n\vec{a}_1 + m\vec{a}_2, a_{nm} = \|\vec{a}_{nm}|$, n, m are integers, and

$$\begin{aligned} \eta &= \delta^{\mu z}\delta^{\nu z}, \quad \tau = (-1)^{\delta^{\mu z}}(-1)^{\delta^{\nu z}}, \\ \Delta_{pq} &= \mathrm{Erfc}\left(-\frac{ik_{pq}}{2F}\right), \quad \Sigma_{pq} = \frac{i4F}{\sqrt{\pi}}\exp\left(\frac{k_{pq}^2}{4F^2}\right), \\ \Gamma_{nm}^{(1)} &= \exp\left(-ik_0a_{nm}\right)\mathrm{Erfc}\left(a_{nm}F - \frac{ik_0}{2F}\right), \\ \Gamma_{nm}^{(2)} &= -1 - ik_0a_{nm} + k_0^2a_{nm}^2, \\ \Gamma_{nm}^{(3)} &= -k_0^2 + \frac{3ik_0}{a_{nm}} + \frac{3}{a_{nm}^2}, \\ \Gamma_{nm}^{(4)} &= \frac{2F}{\sqrt{\pi}}\exp\left(-F^2a_{nm}^2 + \frac{k_0^2}{4F^2}\right), \\ \Gamma_{nm}^{(5)} &= \frac{3}{a_{nm}} + 2F^2a_{nm}, \quad F = \sqrt{\pi/\left|\vec{a}_1 \times \vec{a}_2\right|}. \end{aligned} \quad \text{(A7)}$$

The convergence of the sums from (A5) is determined by parameter F measured in reciprocal-length units. This parameter has no physical meaning and should be a real positive quantity. The substitution of the value of F into (A7) yields the maximum values of indices (m, n) and (p, q) that are necessary for calculation of lattice sums with a preassigned accuracy. Taking into account that, at large

values of the argument, the equality $\mathrm{Erfc}(x) = \exp(-x^2)/(x\sqrt{\pi})$ holds, we obtain the following condition:

$$\exp\left(-\pi a_{nm}^2 / \left|\vec{a}_1 \times \vec{a}_2\right|\right) \approx \xi, \tag{A8}$$

where ξ is a small quantity determining the calculation accuracy. The exact numerical calculation for a square lattice shows that, when indices (m, n) and (p, q) vary from -2 to 2, the lattice sums are calculated with an accuracy of about $10^{-4}\%$, which is in a good agreement with estimate (A8).

REFERENCES

1. Visimax Technologies, Twinsburg, Ohio, http://visimaxtechnologies.com/anti-reflection-visiclear/.
2. Walheim, S., E. Schaffer, J. Mlynek, and U. Steiner, "Surface-induced structure formation of polymer blends on patterned substrates," *Science*, Vol. 283, 520, 1999.
3. Lalanne, P. and G. M. Morris, "Antireflection behavior of silicon subwavelength periodic structures for visible light," *Nanotechnology*, Vol. 8, 53, 1997.
4. Koenig, G. A. and N. G. Niejelow, "Ultra low residual reflection, low stress lens coating," United States Patent, No. US 7311938 B2, Dec. 25, 2007.
5. Huang, Y.-F., S. Chattopadhyay, Y.-J. Jen, C.-Y. Peng, T.-A. Liu, Y.-K. Hsu, C.-L. Pan, H.-C. Lo, C. H. Hsu, Y. H. Chang, C.-S. Lee, K.-H. Chen, and L.-C. Chen, "Improved broadband and quasi-omnidirectional antireflection properties with biomimetic silicon nanostructures," *Nat. Nanotechnol.*, Vol. 2, 770, 2007.
6. Li, Y., J. Zhang, S. Zhu, H. Dong, Z. Wang, Z. Sun, J. Guo, and B. Yang, "Bioinspired silicon hollow-tip arrays for high performance broadband anti-reflective and water-repellent coatings," *J. Mater. Chem.*, Vol. 19, 1806, 2009.
7. Wang, S., X. Z. Yu, and H. T. Fan, "Simple lithographic approach for subwavelength structure antireflectio," *Appl. Phys. Lett.*, Vol. 91, 061105, 2007.
8. Gombert, A., W. Glaubitt, K. Rose, J. Dreibholz, B. Blasi, A. Heinzel, D. Sporn, W. Doll, and V. Wittwer, "Subwavelength-structured antireflective surfaces on glass," *Thin Solid Films*, Vol. 351, 73, 1999.
9. Wu, Z., J. Walish, A. Nolte, L. Zhai, R. E. Cohen, and M. F. Rubner, "Deformable antireflection coatings from polymer and nanoparticle multilayers," *Adv. Mater.*, Vol. 18, 2699, 2006.

10. Koo, H. Y., D. K. Yi, S. J. Yoo, and D.-Y. Kim, "Snowman-like array of colloidal dimers for antireflecting surfaces," *Adv. Mater.*, Vol. 16, 274, 2004.
11. Ramm, A. G., "Electromagnetic wave scattering by a thin layer in which many small particles are embedded," *Progress In Electromagnetics Research Letters*, Vol. 19, 147–154, 2010.
12. Xi, J.-Q., F. M. Schubert, J. K. Kim, et al., "Optical thin-film materials with low refractive index for broadband elimination of Fresnel reflection," *Nature Photonics*, Vol. 1, 176, 2007.
13. Garcia-Vidal, F. J., "Metamaterials-Towards the dark side," *Nature Photonics*, Vol. 2, 215, 2008.
14. Shalin, A. S. and S. G. Moiseev, "Controlling interface reflectance by a monolayer of nanoparticles," *Quantum Electron.*, Vol. 39, 1175, 2009.
15. Gadomskii, O. N. and A. S. Shalin, "Effect of optical blooming of a nanocrystal monolayer and the interface between two media," *Journal of Experimental and Theoretical Physics*, Vol. 105, No. 4, 761, 2007.
16. Yanagishita, T., K. Nishio, and H. Masuda, "Anti-reflection structures on lenses by nanoimprinting," *Using Ordered Anodic Porous Alumina Appl. Phys. Express*, Vol. 2, 022001, 2009.
17. Mishchenko, M. I., L. D. Travis, and A. A. Lacis, *Scattering, Absorption and Emission of Light by Small Particles*, Cambridge University Press, Cambridge, 2002.
18. Haarmans, M. T. and D. Bedeaux, "The polarizability and the optical properties of lattices and random distributions of small metal spheres on a substrate," *Thin Solid Films*, Vol. 224, 117, 1993.
19. Mie, G., "Beiträge zur Optik trüber medien, speziell kolloidaler metallösungen," *Ann. Phys.*, Vol. 25, 377, 1908.
20. Shalin, A. S., "Effect of the absolute transparency of an ordered nanocomposite," *JETP Lett.*, Vol. 90, 257, 2009.
21. Shalin, A. S., "Broadband blooming of a medium modified by an incorporated layer of nanocavities," *JETP Lett.*, Vol. 91, 637, 2010.
22. Arfken, G. B. and H. J. Weber, *Mathematical Methods for Physicists*, Acad. Press, New York, 1995.
23. Fleming, A. H. J., "A finite element method for composite scatterers," *Progress In Electromagnetics Research*, Vol. 2, 69–112, 1990.
24. Zhai, Y.-B. and T.-J. Cui, "Three-dimensional axisymmetric

invisibility cloaks with arbitrary shapes in layered-medium background," *Progress In Electromagnetics Research B*, Vol. 27, 151–163, 2011.

25. Taflove, A. and S. C. Hagness, *Computational Electrodynamics: The Finite-difference Time-Domain Method*, Artech House, Boston, 2000.
26. Prather, D. W. and S. Shi, "Formulation and application of the finite-difference time-domain method for the analysis of axially symmetric diffractive optical elements," *Opt. Soc. Am. A*, Vol. 16, 1131, 1999.
27. Lin, Z., X. Zhang, and G. Fang, "Theoretical model of electromagnetic scattering from 3D multi-layer dielectric media with slightly rough surfaces," *Progress In Electromagnetics Research*, Vol. 96, 37–62, 2009.
28. Curry, A., G. Nusz, A. Chilkoti, and A. Wax, "Substrate effect on refractive index dependence of plasmon resonance for individual silver nanoparticles observed using darkfield microspectroscopy," *Opt. Express*, Vol. 13, 2668, 2005.
29. Shalin, A. S. and S. G. Moiseev, "Optical properties of nanostructured layers on the surface of an underlying medium," *Optics and Spectroscopy*, Vol. 106, No. 6, 916, 2009.
30. Born, M. and E. Wolf, *Principles of Optics*, Pergamon, Oxford, 1969.
31. Zhang, G.-H., M. Xia, and C. H. Chan, "Time domain integral equation approach for analysis of transient responses by metallic-dielectric composite bodies," *Progress In Electromagnetics Research*, Vol. 87, 1–14, 2008.
32. Ylä-Oijala, P., M. Taskinen, and J. Sarvas, "Surface integral equation method for general composite metallic and dielectric structures with junctions," *Progress In Electromagnetics Research*, Vol. 52, 81–108, 2005.
33. COMSOL Multiphysics 3.4, COMSOL AB, Stockholm, Sweden; http://www.comsol.com/products/multiphysics/.
34. Bohren, C. F. and D. R. Huffman, *Absorption and Scattering of Light by Small Particles*, Wiley, New York, 1983.
35. Evlyukhin, A. B. and S. I. Bozhevolnyi, "Point-dipole approximation for surface plasmon polariton scattering: Implications and limitations," *Phys. Rev. B.* Vol. 71, 134304, 2005.
36. Gadomskii, O. N. and A. S. Shalin, "Optical near-field resonances in the system of interacting nanoparticles," *The Physics of Metals and Metallography*, Vol. 101, No. 5, 425, 2006.

37. Poppe, G. P. M., C. M. J. Wijers, and A. Silfhout, "Ir spectroscopy of CO physisorbed on NaCl (100): Microscopic treatment," *Phys. Rev. B*, Vol. 44, No. 15, 7917–7929, 1991.
38. Wijers, C. M. J. and G. P. M. Poppe, "Microscopic treatment of the angular dependence of surface induced optical anisotropy," *Phys. Rev. B*, Vol. 46, No. 2, 7605–7620, 1992.
39. Milton, G. W., *The Theory of Composites*, Cambridge University Press, Cambridge, 2004.
40. Zaimidoroga, O. A., V. N. Samoilov, and I. E. Protsenko, "The problem of realization of a high refractive index and the optical properties of heterogeneous media," *Phys. Part. Nucl.*, Vol. 33, 52, 2002.
41. Palik, E. D., *Handbook of Optical Constants of Solids*, Academic Press, New York, 1985.
42. Song, Y. M., H. J. Choi, J. S. Yu, and Y. T. Lee, "Design of highly transparent glasses with broadband antireflective subwavelength structures," *Opt. Express*, Vol. 18, No. 12, 13063, 2010.
43. Xi, J.-Q., J. K. Kim, E. F. Schubert, D. Ye, T.-M. Lu, S.-Y. Lin, and J. S. Juneja, "Very low-refractive-index optical thin films consisting of an array of SiO2 nanorods," *Opt. Lett.*, Vol. 31, No. 5, 601, 2006.